JOURNAL OF SOLID STATE CHEMISTRY 66, 293–303 (1987)

$M_4Se_{16}Br_2$ (M = Nb, Ta), a New Chain-like Structure from Progressive Condensation of (M_2Se_4) Groups

P. GRENOUILLEAU, A. MEERSCHAUT,* L. GUEMAS, AND J. ROUXEL

Laboratoire de Chimie des Solides, U.A. 279, 2, rue de la Houssinière, 44072 Nantes Cédex, France

Received March 5, 1986; in revised form June 3, 1986

$Nb_4Se_{16}Br_2$ and $Ta_4Se_{16}Br_2$ crystallize in the monoclinic system, space group $P2_1/c$ with a = 12.862(3) Å, b = 13.862(3) Å, c = 16.029(3) Å, β = 127.70(1)°, Z = 4 and a = 12.844(2) Å, b = 13.875(2) Å, c = 16.018(4) Å, β = 127.57(1)°, Z = 4, respectively. The structures were solved from 3182 and 2784 reflections, respectively, collected on a NONIUS CAD4 automatic diffractometer (Mo$K\alpha$ radiation). The final R indexes are 0.030 and 0.033. The common structural type is based on the presence of four chains running in a direction parallel to the a axis. Along the chains four metal atoms are found; short and long M–M distances alternate in the sequence of three consecutive short bonds ($\bar{d}(M\text{–}M) \simeq 3.1$ Å) and one long ($\bar{d}(M \ldots M) \simeq 3.7$ Å). The shortest bonds are associated with [M_4Se_{12}] groups built up from the condensation of three [M_2Se_4] units.

Introduction

The $(MSe_4)_nI$ series of derivatives (M = Nb, Ta; n = 2, 3, 10/3) are pseudo-one-dimensional compounds which may present very interesting electrical properties in relation to charge density wave-type instabilities (*1*, *2*). Such striking properties have stimulated numerous chemical attempts to change n values (iodine content) with the aim of getting new materials with similar transport properties.

The common structural type is built up from [MSe_4] chains (with a rectangular antiprismatic coordination of M by two (Se_4) rectangles) and iodine columns that both run parallel to the c axis of a tetragonal unit cell. This arrangement is reminiscent of some organic salts such as TSeT–I_x (TSeT = tetraselenotetracene) in which TSeT stackings are separated by iodine columns (*3*). Many works in that field have dealt with an exchange of the iodine counter-ions (it is more often I_3^- than I^- in that case), particularly by other halogen or pseudo-halogen species.

In the case of $(MSe_4)_nI$ phases there were two reasons to focus on the halogen column:

(i) In the case of a simple exchange of iodine by bromine or chlorine, it can be predicted that the structures will be less stable due to a change in electronegativity and size of the halogen. Indeed, the overall charge on the [MX_4] chains will increase, the halogen itself being more electronegative. These chains, at the same time, may not be sufficiently separated by a smaller halogen to keep a stable organization relative to each other.

* To whom all correspondence should be addressed.

0022-4596/87 $3.00

(ii) A new structural arrangement could be observed in which the halogen, due to its increased electronegativity, will tend to be directly bonded to the metal.

In this work both possibilities have been tested. Up to now, a direct replacement of iodine by chlorine or bromine has been unsuccessful. $(MSe_4)_nI$ phases react at room temperature with chlorine diluted in argon. ICl and ICl_3 are formed as expected due to the more electronegative character of chlorine. But the structural organization is destroyed (no X-ray diagram). Furthermore, selenium chloride is also formed, indicating a reaction between $[MSe_4]$ chains and chlorine, and not only a simple exchange reaction with iodine. Use of milder chlorinating reagents has been studied, but it led to unstable compounds.

The second possibility, tackled through chemical reaction at higher temperature, has led to interesting new phases. In spite of their formula $M_4Se_{16}Br_2$ (M = Nb, Ta), which could be expressed $(MSe_4)_2Br$, they show a new structural type.

Experimental

Single crystals of $Nb_4Se_{16}Br_2$ and $Ta_4Se_{16}Br_2$ were prepared by mixing the appropriate quantities of Nb/Ta, Se, and Br_2 in a Pyrex tube sealed under vacuum. The Pyrex tube was heated for 15 days in a temperature gradient (500–460°C) and then slowly cooled to room temperature (1 day). Needle-shaped crystals are formed at the cold end of the tube. A microanalysis of single crystals was made with a scanning electron microscope (Microsonde OUEST-CNEXO) employing energy selection of the X-ray spectrum emitted by the specimen. Experimental and theoretical values for each compound ae reported in Tables IA and IB.

A preliminary X-ray study (Weissenberg and precession photographs) revealed that the crystals belong to the Laue group $2/m$.

TABLE IA

EXPERIMENTAL AND THEORETICAL VALUES FOR $Nb_4Se_{16}Br_2$

1. *Physical, crystallographic, and analytical data*
Formula: $Nb_4Se_{16}Br_2$ Molecular weight: 1794.8
Theoretical weight fraction concentration (%): Nb, 20.7; Se, 70.4; Br, 8.9
Microprobe analysis, average on 20 analysis points (%): Nb, 18.9; Se, 74.0; Br, 7.1
Crystal symmetry: monoclinic Space group: $P2_1/c$
Cell parameters (293 K): a = 12.862(3) Å, b = 13.862(3) Å; c = 16.029(3) Å; β = 127.70(1)°; V = 2261.1 Å^3; Z = 4
Density: d_{calc} = 5.236
Absorption factor: $\mu(\lambda MoK\alpha)$, 307 cm^{-1}
Crystal size: 0.02 × 0.05 × 0.4 mm^3

2. *Data collection*
Temperature: 293 K Radiation: Mo$K\alpha$
Monochromator: oriented graphite (002) Scan mode: ω
Recording angle range: $2° < \theta < 35°$ Scan angle: $0.85 + 0.35 \tan\theta$
Values determining the scan speed: SIGPRE, 0.60; SIGMA, 0.01; VPRE, 20° min^{-1}; TMAX = 100 sec
Standard reflection: 5 1 7, 0 1 6, 0 4 6 Periodicity: 3600 sec

3. *Refinement conditions*
Reflections for the refinement of the cell dimensions: 25
Utilized reflections: 3182 with $I > 4\sigma(I)$ ESD = 6.437
Refined parameters: 203
Reliability factors:

$$R = \Sigma\big||F_o| - |F_c|\big|/\Sigma|F_o|$$

$$R_w = [\Sigma w(|F_o| - |F_c|)^2/\Sigma wF_o^2]^{1/2}$$

4. *Refinement results*
R = 0.030 R_w = 0.036 with w = 1
Extinction coefficient: $E_c = 2.77\ 10^{-8}$
Difference Fourier maximum peak intensity: 1.67 e^-/Å^3

The systematic absences ($0k0$, $k = 2n + 1$ and $h0l$, $l = 2n + 1$) are indicative of space group $P2_1/c$.

Lattice constants are refined from a carefully indexed Guinier powder pattern (see Tables IIA and IIB) using Cu$K\alpha_1$ strictly

TABLE IB

EXPERIMENTAL AND THEORETICAL VALUES FOR $Ta_4Se_{16}Br_2$

1. *Physical, crystallographic, and analytical data*
Formula: $Ta_4Se_{16}Br_2$ Molecular weight: 2147
Theoretical weight fraction concentration (%): Ta, 33.7; Se, 58.9; Br, 7.4
Microprobe analysis, average on 4 analysis points (%): Ta, 34.1; Se, 58.9; Br, 7.0
Crystal symmetry: monoclinic Space group: $P2_1/c$
Cell parameters (293 K): a = 12.844(2) Å, b = 13.875(2) Å; c = 16.018(4) Å; β = 127.57(1)°; V = 2262 Å^3; Z = 4
Density: d_{calc} = 6.34 d_{obs} = 6.28
Absorption factor: $\mu(\lambda MoK\alpha)$, 480 cm^{-1}
Crystal size: 0.01 × 0.012 × 0.52 mm^3

2. *Data collection*
Temperature: 293 K Radiation: Mo$K\alpha$
Monochromator: oriented graphite (002) Scan mode: $\omega/2\theta$
Recording angle range: $2° < \theta < 37°$ Scan angle: 1.40 + 0.60 tan θ
Values determining the scan speed: SIGPRE, 0.60; SIGMA, 0.015; VPRE, 7° min^{-1}; TMAX = 100 sec
Standard reflection: $\bar{2}$ 6 4, $\bar{4}$ 0 10, 4 $\bar{4}$ 8 Periodicity: 3600 sec

3. *Refinement conditions*
Reflections for the refinement of the cell dimensions: 25
Utilized reflections: 2784 with $I > 4\sigma(I)$
Refined parameters: 203
Reliability factors:

$$R = \Sigma\big||F_o| - |F_c|\big|/\Sigma|F_o|$$
$$R_w = [\Sigma w(|F_o| - |F_c|)^2/\Sigma wF_o^2]^{1/2}$$

4. *Refinement results*
R = 0.033 R_w = 0.038 with w = 1
Extinction coefficient: $E_c = 2.89\ 10^{-8}$
Difference Fourier maximum peak intensity: 2.1 e^-/Å^3

TABLE IIA

$Nb_4Se_{16}Br_2$—X-RAY POWDER DIFFRACTION DATA

$h\ k\ l$	d_{obs} (Å)	d_{calc} (Å)	$I/I_0{}^a$	$h\ k\ l$	d_{obs} (Å)	d_{calc} (Å)	$I/I_0{}^a$
0 1 1	9.33	9.36	27	2 3 2	2.5986	2.5973	16
0 0 2	6.332	6.341	422	3 4 $\bar{1}$		2.5998	16
0 2 1	6.070	6.082	1000	4 3 $\bar{2}$	2.5776	2.5786	7
2 0 $\bar{4}$	4.003	4.007	12	4 0 $\bar{6}$		2.5774	85
1 3 $\bar{2}$		4.003	38	1 1 4	2.5616	2.5629	43
2 1 $\bar{4}$	3.849	3.849	56	4 0 0	2.5443	2.5441	121
3 1 $\bar{1}$	3.779	3.782	9	3 4 $\bar{4}$	2.5315	2.5324	84
1 3 1	3.720	3.722	75	3 2 $\bar{6}$	2.4937	2.4925	24
1 2 2	3.662	3.669	11	3 3 1	2.4384	2.4369	31
1 1 $\bar{4}$	3.615	3.617	16	1 2 4		2.4408	21
2 2 $\bar{4}$	3.471	3.469	44	3 1 2	2.3979	2.3984	20
2 3 $\bar{3}$	3.446	3.439	8	0 2 5	2.3814	2.3820	15
1 3 $\bar{3}$		3.450	15	5 0 $\bar{6}$	2.3534	2.3510	28
3 1 0	3.2948	3.2949	96	1 1 $\bar{6}$	2.3481	2.3452	45
3 2 $\bar{4}$	3.2717	3.2707	33	0 4 4	2.3390	2.3393	87
1 1 3	3.1740	3.1742	41	4 4 $\bar{4}$	2.3199	2.3211	27
4 0 $\bar{2}$	3.1079	3.1075	380	0 5 3		2.3184	171
3 3 $\bar{3}$	3.0952	3.0948	113	5 1 6	2.3153	2.3178	24
3 1 $\bar{5}$	3.0816	3.0803	82	4 4 $\bar{2}$		2.3136	177
4 1 $\bar{2}$	3.0299	3.0310	23	0 6 1	2.2737	2.2730	67
2 4 $\bar{2}$		3.0322	25	1 6 $\bar{1}$		2.2719	22
2 3 $\bar{4}$		3.0272	13	1 2 $\bar{6}$	2.2500	2.2505	33
2 4 $\bar{1}$		3.0268	15	4 3 0	2.2289	2.2286	13
2 3 1	3.0035	3.0065	4	2 0 4	2.1617	2.1621	22
4 2 $\bar{3}$	2.9159	2.9166	15	4 2 $\bar{7}$	2.1558	2.1586	46
3 2 $\bar{5}$	2.8738	2.8747	35	4 2 1	2.1358	2.1347	105
2 4 $\bar{3}$		2.8750	60	1 3 $\bar{6}$	2.1160	2.1154	44
2 2 2	2.8612	2.8604	98	2 6 0	2.1026	2.1037	48
3 4 $\bar{3}$	2.6623	2.6647	117	0 1 6	2.0911	2.0896	24
4 2 $\bar{5}$		2.6611	36	3 1 3	2.0715	2.0701	21
4 2 $\bar{1}$	2.6384	2.6386	104	4 4 $\bar{6}$	2.0649	2.0666	43
1 5 $\bar{2}$	2.6237	2.6201	22	4 4 0	2.0511	2.0508	93
2 3 $\bar{5}$	2.6170	2.6160	21	1 1 $\bar{7}$	1.9869	1.9874	25
2 4 1	2.6071	2.6077	74	4 0 2	1.9787	1.9796	31

[a] The intensities are calculated from the Lazy Pulverix program (*12*).

monochromatized radiation, λ = 1.54056. Silicon (a = 5.43106 Å) was used as an internal standard. The resulting lattice constants are:

$Nb_4Se_{16}Br_2$ a = 12.862(3)Å,
b = 13.862(3)Å, c = 16.029(3)Å,
β = 127.70(1)°, V = 2261 Å^3,

$Ta_4Se_{16}Br_2$ a = 12.844(2)Å,
b = 13.875(2)Å, c = 16.018(4)Å,
β = 127.57(1)°, V = 2262 Å^3.

The a direction corresponds to the growing axis of the crystals.

Single-crystal X-ray data were recorded with an automated four-circle ENRAF-NONIUS CAD4 diffractometer with graphite monochromated Mo$K\alpha$ radiation. The experimental conditions used to collect the data are summarized in Tables IA and B. An absorption correction was applied to both sets of data. Lorentz and polarization effects were taken into account as usual.

TABLE IIB

$Ta_4Se_{16}Br_2$—X-RAY POWDER DIFFRACTION DATA

h k l	d_{obs} (Å)	d_{calc} (Å)	I/I_0[a]	h k l	d_{obs} (Å)	d_{calc} (Å)	I/I_0[a]
1 0 0	10.21	10.18	7	3 2 $\bar{6}$	2.4927	2.4912	10
0 1 1	9.35	9.37	22	3 3 1	2.4406	2.4391	19
1 0 $\bar{2}$	8.004	8.008	21	3 1 2	2.4016	2.4011	16
1 1 $\bar{2}$	6.926	6.935	23	0 2 5	2.3838	2.3846	21
0 0 2	6.345	6.348	448	5 0 $\bar{6}$	2.3475	2.3471	18
0 2 1	6.080	6.088	1000	1 1 $\bar{6}$		2.3468	36
1 0 2	4.322	4.330	10	0 4 4	2.3434	2.3417	70
1 2 $\bar{3}$	4.147	4.154	17	0 5 3	2.3193	2.3206	19
1 3 $\bar{2}$	4.007	4.005	21	4 4 $\bar{4}$		2.3199	134
2 0 $\bar{4}$		4.004	7	5 1 $\bar{6}$	2.3141	2.3142	19
2 1 $\bar{4}$	3.844	3.847	32	4 4 $\bar{2}$		2.3135	147
1 3 1	3.725	3.726	29	0 6 1	2.2748	2.2750	69
0 2 3	3.611	3.613	25	1 2 $\bar{6}$	2.2497	2.2522	17
0 4 0	3.467	3.469	12	2 3 3		2.2486	24
2 2 $\bar{4}$		3.468	21	5 2 $\bar{6}$	2.2229	2.2233	15
3 1 0	3.2960	3.2964	47	1 6 $\bar{2}$		2.2217	8
3 2 $\bar{4}$	3.2711	3.2675	17	5 3 $\bar{5}$	2.1964	2.1969	9
1 1 3	3.1790	3.1786	18	4 2 $\bar{7}$	2.1560	2.1568	38
4 0 $\bar{2}$	3.1069	3.1051	29	4 2 1	2.1353	2.1364	88
3 3 $\bar{3}$	3.0926	3.0932	51	1 3 $\bar{6}$	2.1170	2.1170	36
3 1 $\bar{5}$	3.0775	3.0772	30	2 6 0	2.1054	2.1054	27
2 4 $\bar{1}$	3.0284	3.0283	10	5 3 $\bar{6}$	2.0918	2.0930	9
4 2 $\bar{3}$	2.9131	2.9139	49	0 1 6		2.0919	13
3 2 $\bar{5}$	2.8733	2.8725	26	3 1 3	2.0724	2.0727	17
2 2 2	2.8652	2.8639	41	4 4 0	2.0516	2.0520	81
4 2 $\bar{5}$	2.6600	2.6578	109	0 6 3	2.0297	2.0293	36
4 2 $\bar{1}$	2.6387	2.6387	110	1 5 $\bar{5}$	2.0103	2.0103	19
1 5 $\bar{2}$	2.6215	2.6220	12	1 1 $\bar{7}$	1.9886	1.9890	26
3 1 $\bar{6}$		2.6212	17	4 0 2	1.9820	1.9816	26
2 4 1	2.6096	2.6102	37	1 6 $\bar{4}$	1.9667	1.9681	12
4 0 $\bar{6}$	2.5719	2.5710	64	0 7 1	1.9581	1.9584	5
4 0 0	2.5440	2.5451	92	5 1 $\bar{8}$	1.9386	1.9386	12
3 4 $\bar{4}$	2.5332	2.5319	47	0 5 5	1.8742	1.8733	11

[a] The intensities are calculated from the Lazy Pulverix program (*12*).

After averaging equivalent reflections and omitting those for which $I < 4\sigma(I)$, 3182 and 2784 independent reflections were kept for $Nb_4Se_{16}Br_2$ and $Ta_4Se_{16}Br_2$, respectively.

The structure was determined by the deconvolution of the Patterson function and subsequent Fourier difference syntheses. The refinement was carried out by full-matrix least-squares calculations. Conventional atomic scattering factors (*4*) were used and corrected for anomalous dispersion (*5*). An isotropic secondary extinction parameter was also refined (see Table I).

All calculations were performed on a PDP 11/34 computer using the SDP package. The final cycle of refinement of the positional parameters, occupancy factors, and anisotropic thermal parameters results in the conventional residuals R and R_w values ($w = 1$)

$R = 0.030, \quad R_w = 0.036$ for $Nb_4Se_{16}Br_2$,

$R = 0.033, \quad R_w = 0.038$ for $Ta_4Se_{16}Br_2$.

The final Fourier difference map shows no value higher than 1.7 and 2.1 $e^-/Å^3$ for $Nb_4Se_{16}Br_2$ and $Ta_4Se_{16}Br_2$, respectively.

Positional and thermal parameters are summarized in Tables III–VI for these two isomorphous compounds. The two sites Se13A and Se13B are too close to each other and correspond to non-fully occupied positions with an occupancy that has been constrained to follow the $(1 - x, x)$ limiting condition. It appears that x is equal to 0.17 for $Nb_4Se_{16}Br_2$ and 0.20 for $Ta_4Se_{16}Br_2$.

TABLE III

$Nb_4Se_{16}Br_2$—POSITIONAL PARAMETERS AND THEIR ESTIMATED STANDARD DEVIATIONS

Atom	Multiplicity	x	y	z	B_{eq} (Å^2)
Nb1	1	−0.00428(9)	0.35911(8)	0.22921(7)	1.21(2)
Nb2	1	0.25439(9)	0.38099(8)	0.24521(7)	1.14(2)
Nb3	1	0.51095(9)	0.39035(8)	0.27124(7)	1.11(2)
Nb4	1	0.78202(9)	0.38654(8)	0.30868(7)	1.12(2)
Se1	1	0.2304 (1)	0.3636 (1)	0.40232(7)	1.50(2)
Se2	1	0.1886 (1)	0.2271 (1)	0.30136(9)	1.57(3)
Se3	1	0.0688 (1)	0.5121 (1)	0.17304(9)	1.74(3)
Se4	1	0.4367 (1)	0.5091 (1)	0.35817(8)	1.55(2)
Se5	1	0.4973 (1)	0.3470 (1)	0.41974(8)	1.47(2)
Se6	1	0.3086 (1)	0.2715 (1)	0.14620(9)	1.50(2)
Se7	1	0.2821 (1)	0.4338 (1)	0.09629(9)	1.71(3)
Se8	1	0.7447 (1)	0.4721 (1)	0.42844(8)	1.46(2)
Se9	1	0.6607 (1)	0.2368 (1)	0.32802(9)	1.60(3)
Se10	1	0.6250 (1)	0.5435 (1)	0.25883(8)	1.41(2)
Se11	1	0.5786 (1)	0.2950 (1)	0.16022(9)	1.54(2)
Se12	1	−0.0006 (1)	0.3699 (1)	0.07026(8)	1.63(3)
Se13A	0.83(2)	0.9447 (1)	0.2511 (1)	0.3407 (1)	1.38(3)
Se13B	0.17(2)	0.9092 (6)	0.2368 (1)	0.2871 (5)	1.38(3)
Se14	1	0.9532 (1)	0.5033 (1)	0.31860(8)	1.38(2)
Se15	1	0.7712 (1)	0.4560 (1)	0.14748(8)	1.32(2)
Se16	1	0.0004 (1)	−0.1685 (1)	0.00791(9)	1.79(3)
Br1	1	0.4729 (1)	0.6283 (1)	0.0460 (1)	2.52(3)
Br2	1	0.1637 (1)	0.7125 (1)	0.38285(9)	1.91(3)

Note. $B_{eq} = \frac{4}{3}\Sigma_i\Sigma_j\beta_{ij}a_ia_j$.

TABLE IV

$Nb_4Se_{16}Br_2$—GENERAL TEMPERATURE FACTOR EXPRESSIONS, U's

Atom	U_{11}	U_{22}	U_{33}	U_{12}	U_{13}	U_{23}
Nb1	0.0144(3)	0.0104(4)	0.0202(3)	0.0000(3)	0.0102(2)	−0.0004(4)
Nb2	0.0136(3)	0.0127(5)	0.0160(3)	0.0005(3)	0.0086(2)	−0.0004(3)
Nb3	0.0133(3)	0.0137(4)	0.0148(3)	−0.0007(3)	0.0083(2)	−0.0009(4)
Nb4	0.0133(3)	0.0113(4)	0.0157(3)	0.0001(3)	0.0078(2)	0.0003(4)
Se1	0.0188(3)	0.0190(6)	0.0193(4)	−0.0011(4)	0.0117(2)	−0.0008(4)
Se2	0.0189(4)	0.0127(5)	0.0270(4)	0.0016(4)	0.0136(3)	0.0016(4)
Se3	0.0243(4)	0.0120(5)	0.0318(4)	0.0025(4)	0.0181(3)	0.0037(4)
Se4	0.0206(4)	0.0160(6)	0.0229(4)	−0.0030(4)	0.0137(2)	−0.0049(4)
Se5	0.0167(4)	0.0208(6)	0.0150(3)	0.0013(4)	0.0081(2)	0.0013(4)
Se6	0.0169(4)	0.0176(6)	0.0212(4)	−0.0033(4)	0.0111(2)	−0.0057(4)
Se7	0.0188(4)	0.0253(6)	0.0183(4)	0.0029(5)	0.0100(3)	0.0047(4)
Se8	0.0176(4)	0.0173(6)	0.0165(4)	−0.0014(4)	0.0084(2)	−0.0033(4)
Se9	0.0210(4)	0.0136(6)	0.0269(4)	0.0012(4)	0.0151(2)	0.0026(4)
Se10	0.0182(4)	0.0133(5)	0.0216(4)	0.0002(4)	0.0119(2)	0.0009(4)
Se11	0.0191(4)	0.0196(6)	0.0215(4)	−0.0043(4)	0.0133(2)	−0.0069(4)
Se12	0.0172(4)	0.0234(6)	0.0182(4)	0.0007(4)	0.0093(2)	0.0019(5)
Se13A Se13B	0.0202(4)	0.0103(6)	0.0276(5)	0.0008(4)	0.0175(3)	0.0017(5)
Se14	0.0172(3)	0.0118(5)	0.0223(4)	−0.0030(4)	0.0115(2)	−0.0031(4)
Se15	0.0163(3)	0.0152(5)	0.0176(3)	0.0022(4)	0.0099(2)	0.0012(4)
Se16	0.0206(4)	0.0232(6)	0.0189(4)	−0.0034(5)	0.0093(3)	−0.0041(4)
Br1	0.0357(6)	0.0257(7)	0.0195(5)	−0.0010(6)	0.0094(4)	0.0006(5)
Br2	0.0219(4)	0.0194(6)	0.0286(4)	0.0035(4)	0.0140(3)	0.0073(5)

Note. The form of the anisotropic thermal parameter is: $\exp[-2\pi^2(h^2a^{*2}U_{11} + k^2b^{*2}U_{22} + l^2c^{*2}U_{33} + 2hka^*b^*U_{12} + 2hla^*c^*U_{13} + 2klb^*c^*U_{23})]$, where a^*, b^*, and c^* are reciprocal lattice constants.

Crystal Structure Description

Figure 1 displays a projection of the crystal structure in the (a, b) plane and Fig. 2 shows a projection in the (a, c) plane. The structure exhibits waved, or broken, types of chains running in a direction parallel to the a axis (see Fig. 3). Along the chains four metal atoms are found within one a parameter. Short and long M–M distances alternate in the sequence of three consecutive short distances (Nb1–Nb2 = 3.202(1) Å, Nb2–Nb3 = 3.076(1) Å, Nb3–Nb4 = 3.167(1) Å, and similarly, Ta1–Ta2 = 3.187(1) Å, Ta2–Ta3 = 3.055(1) Å, Ta3–Ta4 = 3.153(1) Å), and a long one (Nb4–Nb1 = 3.702(1) Å and Ta4–Ta1 = 3.683(1) Å). Tables VIIA and VIIB summarize the main interatomic distances within each [MSe$_8$] polyhedron as described below. Indeed, $M2$ and $M3$ are surrounded by a rectangular antiprism of selenium atoms. This coordination is designed by two (Se_4) rectangles, each of them being built from two $(Se_2)^{2-}$ pairs ($d_{Se-Se} \simeq 2.35$ Å). The situation is more complicated for $M1$ and $M4$ environments. Each of these atoms has on one side a (Se_4) rectangle which separates them from $M2$ or $M3$, respectively, but between them one finds a true selenium pair (Se14–S15) and a complex situation which refers to the Se16, Se13A, Se13B, and Br2 positions. Se13A and Se13B positions are mutually exclusive ($d_{Se13A-Se13B} = 0.719$ Å). They are always occupied by selenium but with respective occupation rates of 5/6 and 1/6.

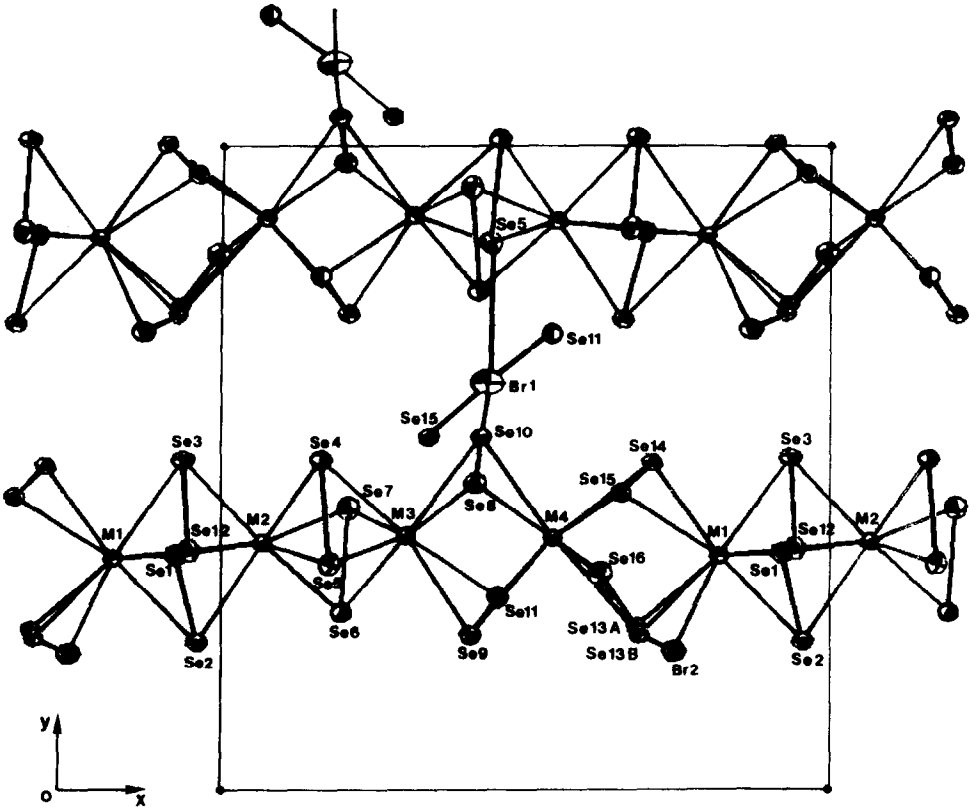

FIG. 1. Projection onto the (*a*, *b*) plane.

Let us examine the $Nb_4Se_{16}Br_2$ compound. If Se13A is occupied (5/6), in connection with a bond length Se16–Se13A = 2.357 Å, the Se16 atomic position is made of selenium (5/6) building a true $(Se_2)^{2-}$ pair. At the same moment the Br2 position is occupied by bromine (5/6) with a Se13A–Br2 distance = 2.998 Å (which fits well with Br–Se $\simeq$ 3.1 Å in $Nb_6Se_{20}Br_6$ (*6*)). If Se13B is occupied (1/6) then Se16 is populated by bromine (1/6) with Se13B–"Se16" = 3.039 Å, and Br2 is occupied by selenium, forming once more a $(Se_2)^{2-}$ pair (Se13B–"Br2" = 2.304 Å). This is summarized in the schematic view (Fig. 4). In any case, *M*1 and and *M*4 are separated by two selenium pairs (Se14–Se15 and either Se16–Se13A for 5/6 or Se13B–Br2 (selenium part) for 1/6) and a bromine atom.

A similar situation occurs for $Ta_4Se_{16}Br_2$ except that the occupation rate was refined to $x = 0.20$, leading to Se13A (4/5) and Se13B (1/5).

The other bromine atom (Br1) exhibits a particular role quite similar to that exercised by iodine in the $(MSe_4)_nI$ series. Let us recall that iodine was shared between four chains through four I–Se bond lengths of 3.278 Å. Selenium atoms presented a squared arrangement around iodine (*1*).

In the $M_4Se_{16}Br_2$ compounds, Br1 is connected to four selenium atoms belonging to three different chains (see Tables VIIa and VIIb). However, the four chains within the unit cell are interconnected via both bromine atoms Br1 and Br1C (see Figs. 1 and 2).

That situation is unique in the $M_4Se_{16}Br_2$

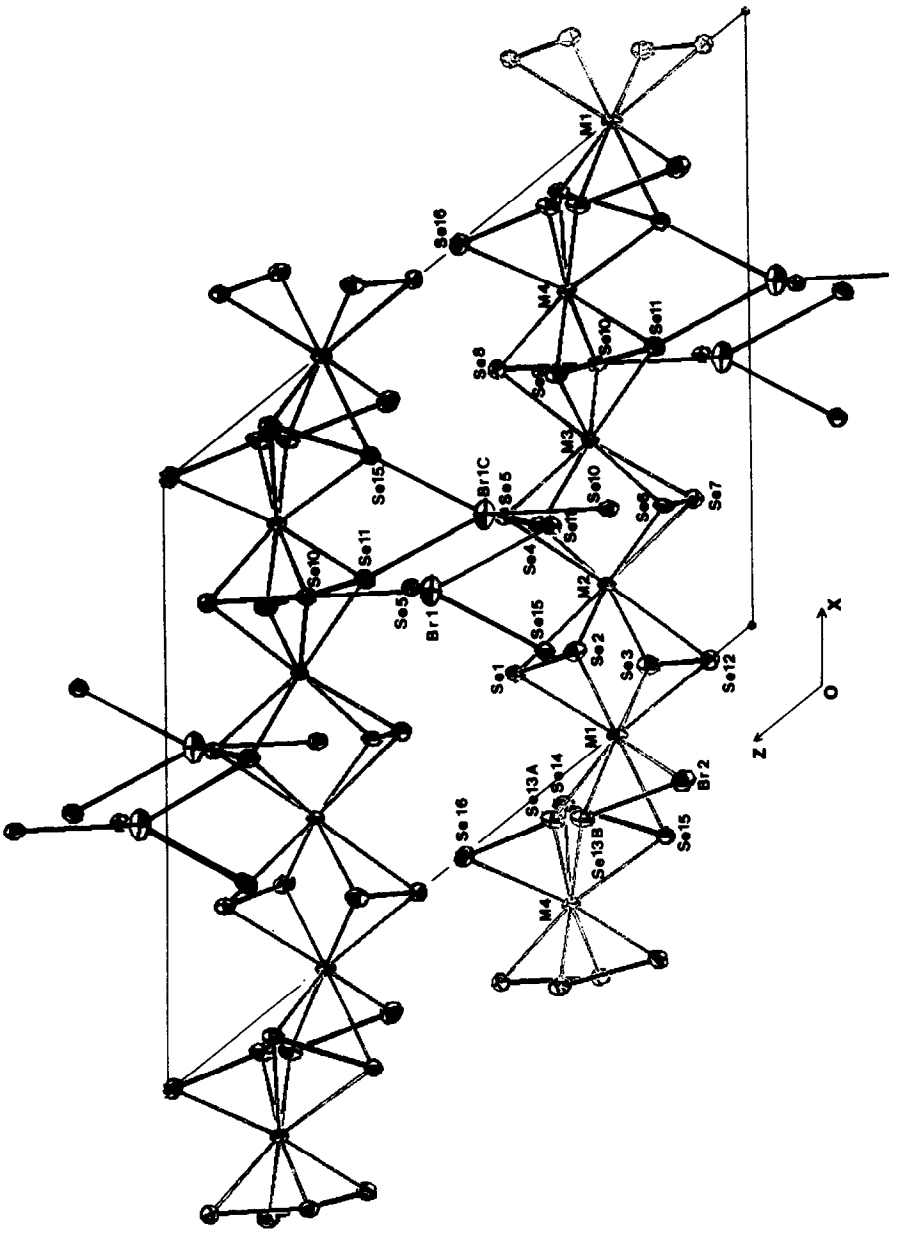

FIG. 2. Projection onto the (a, c) plane.

TABLE V

$Ta_4Se_{16}Br_2$—POSITIONAL PARAMETERS AND THEIR ESTIMATED STANDARD DEVIATIONS

Atom	Multiplicity	x	y	z	B_{eq} (Å^2)
Ta1	1	−0.00445(6)	0.35927(6)	0.22920(5)	1.01(1)
Ta2	1	0.25481(6)	0.38050(7)	0.24588(5)	0.93(1)
Ta3	1	0.51079(6)	0.38965(6)	0.27172(5)	0.90(1)
Ta4	1	0.78168(6)	0.38598(5)	0.30868(5)	0.94(1)
Se1	1	0.2289 (2)	0.3637 (2)	0.4025 (1)	1.33(4)
Se2	1	0.1877 (2)	0.2268 (2)	0.3007 (2)	1.42(4)
Se3	1	0.0708 (2)	0.5120 (2)	0.1755 (1)	1.49(4)
Se4	1	0.4371 (2)	0.5080 (2)	0.3587 (1)	1.38(4)
Se5	1	0.4970 (2)	0.3449 (2)	0.4198 (1)	1.25(4)
Se6	1	0.3094 (2)	0.2705 (2)	0.1479 (1)	1.28(4)
Se7	1	0.2828 (2)	0.4338 (2)	0.0975 (1)	1.44(4)
Se8	1	0.7441 (2)	0.4707 (2)	0.4287 (1)	1.29(4)
Se9	1	0.6600 (2)	0.2364 (2)	0.3279 (1)	1.38(4)
Se10	1	0.6238 (2)	0.5428 (2)	0.2581 (1)	1.24(4)
Se11	1	0.5777 (2)	0.2961 (2)	0.1596 (1)	1.33(4)
Se12	1	0.0005 (2)	0.3697 (2)	0.0712 (1)	1.43(4)
Se13A	0.80(2)	0.9426 (2)	0.2510 (2)	0.3395 (2)	1.23(4)
Se13B	0.20(2)	0.9070 (8)	0.2402 (8)	0.2893 (7)	1.23(4)
Se14	1	0.9533 (2)	0.5026 (2)	0.3201 (1)	1.21(4)
Se15	1	0.7720 (2)	0.4560 (2)	0.1478 (1)	1.16(4)
Se16	1	0.0025 (2)	−0.1698 (2)	0.0089 (1)	1.55(4)
Br1	1	0.4725 (2)	0.6275 (2)	0.0463 (2)	2.22(5)
Br2	1	0.1633 (2)	0.7141 (2)	0.3831 (2)	1.66(4)

Note. $B_{eq} = \frac{1}{3}\Sigma_i\Sigma_j\beta_{ij}a_ia_j$.

series. For example, bromine atoms were only tightly bonded to niobium atoms in the $Nb_6Se_{20}Br_6$ compound. It can be deduced that both $M_4Se_{16}Br_2$ structures are more "3D" in character than $Nb_6Se_{20}Br_6$ ("2D").

Selenium atoms occur in (Se_2^{2-}) pairs. As bromine atoms are well isolated from each other, they can be regarded as Br^- entities, which would lead us to propose the formal oxidation states $(M^{4+})_2$, $(M^{5+})_2$, $(Se_2^{2-})_8$, $(Br^-)_2$. However, the $M1$–$M2$, $M2$–$M3$, $M3$–$M4$ distances clearly suggest, in regard to what we know about the electronic structure of $(MSe_4)_nI$, that both electrons which could be related to the "M^{4+}" ions are in fact delocalized with the short $M1$–$M2$–$M3$–$M4$ segment. This example of "linear cluster" is the subject of band structure calculations now in progress on all M–Se–Br phases, with a variable length of such units (*7*).

Resistivity measurements performed by a four-probe technique on single crystals of

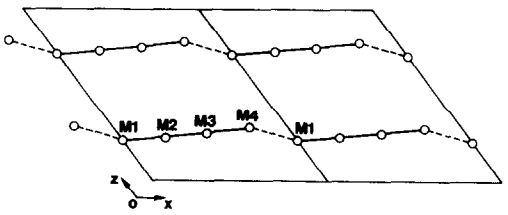

FIG. 3. Schematic view of metallic chains.

both compounds indicate a semiconducting behavior

$Nb_4Se_{16}Br_2$, $E_g = 0.30$ eV

and $Ta_4Se_{16}Br_2$, $E_g = 0.18$ eV

Conclusions and Discussion

The fact that attempts to perform a direct replacement of iodine by bromine in $(MSe_4)_nI$ phases have been unsuccessful sheds some light on stability of the corresponding structural type. It is well known that a layer structure exists to the extent that the van der Waals interactions between the slabs overcome the repulsions between similar anionic layers on each side of these slabs.

In the case of oxides this repulsion is quite strong and very destabilizing and most of the MO_2 oxides have the rutile structure and not the layered structure of the parent MX_2 sulfides or selenides.

On the other hand, the true low-dimen-

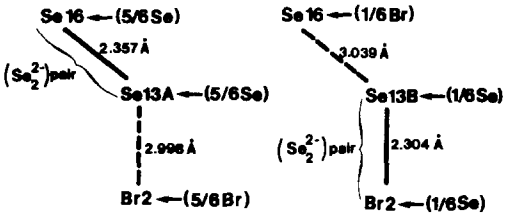

FIG. 4. Schematic view showing the nearest neighboring atoms around Se13A and Se13B in the case of $Nb_4Se_{16}Br_2$.

TABLE VI

$Ta_4Se_{16}Br_2$—GENERAL TEMPERATURE FACTOR EXPRESSIONS, U's

Atom	U_{11}	U_{22}	U_{33}	U_{12}	U_{13}	U_{23}
Ta1	0.0115(2)	0.0117(3)	0.0178(2)	0.0004(3)	0.0103(1)	−0.0001(3)
Ta2	0.0096(2)	0.0140(3)	0.0138(2)	0.0002(2)	0.0081(1)	0.0000(2)
Ta3	0.0098(2)	0.0141(3)	0.0122(2)	−0.0015(3)	0.0077(1)	−0.0016(3)
Ta4	0.0096(2)	0.0122(3)	0.0141(2)	0.0002(3)	0.0073(1)	0.0006(3)
Se1	0.0141(5)	0.022 (1)	0.0181(5)	0.0012(6)	0.0115(3)	−0.0005(7)
Se2	0.0143(5)	0.0160(9)	0.0235(6)	0.0007(6)	0.0115(4)	−0.0002(7)
Se3	0.0192(5)	0.0160(9)	0.0260(6)	0.0027(7)	0.0161(4)	0.0034(7)
Se4	0.0150(5)	0.020 (1)	0.0204(6)	−0.0033(7)	0.0122(4)	−0.0055(7)
Se5	0.0118(5)	0.023 (1)	0.0140(5)	0.0020(6)	0.0082(3)	0.0013(7)
Se6	0.0131(5)	0.0204(9)	0.0198(6)	−0.0046(6)	0.0125(3)	−0.0064(6)
Se7	0.0152(6)	0.024 (1)	0.0165(6)	0.0014(7)	0.0100(4)	0.0027(7)
Se8	0.0142(5)	0.0201(9)	0.0145(6)	−0.0002(6)	0.0087(4)	−0.0017(6)
Se9	0.0155(5)	0.0163(9)	0.0230(6)	−0.0003(6)	0.0130(4)	0.0031(7)
Se10	0.0123(5)	0.0166(9)	0.0187(6)	0.0015(6)	0.0097(4)	0.0011(6)
Se11	0.0183(6)	0.0187(9)	0.0176(5)	−0.0052(6)	0.0130(4)	−0.0055(6)
Se12	0.0135(5)	0.025 (1)	0.0154(6)	0.0006(7)	0.0082(4)	0.0022(7)
Se13A Se13B	0.0202(6)	0.011 (1)	0.0242(7)	0.0026(7)	0.0178(4)	0.0043(8)
Se14	0.0147(5)	0.0149(8)	0.0198(6)	−0.0031(6)	0.0123(3)	−0.0030(6)
Se15	0.0131(5)	0.0164(9)	0.0160(5)	0.0014(6)	0.0096(3)	0.0010(6)
Se16	0.0137(5)	0.025 (1)	0.0173(6)	−0.0026(7)	0.0077(4)	−0.0044(7)
Br1	0.0303(8)	0.026 (1)	0.0179(7)	−0.0012(9)	0.0096(5)	−0.0006(8)
Br2	0.0165(6)	0.020 (1)	0.0246(7)	0.0034(7)	0.0113(4)	0.0079(7)

Note. The form of the anisotropic thermal parameter is: $\exp[-2\pi^2(h^2a^{*2}U_{11} + k^2b^{*2}U_{22} + l^2c^{*2}U_{33} + 2hka^*b^*U_{12} + 2hla^*c^*U_{13} + 2klb^*c^*U_{23})]$, where a^*, b^*, and c^* are reciprocal lattice constants.

sional character decreases when the bonding increases through the van der Waals gap, i.e., when the covalency increases from sulfides to selenides and tellurides. The same features are true for quasi-1D structure. $NbSe_3$ is less one-dimensional than TaS_3. The latter presents important pretransitional effects above the charge density wave transition, illustrating a more important decorrelation between chains. Finally, we come to the conclusion that the more ionic a structure is, the more decorrelated the slabs or chains will be, but at the same time the stability of the structure decreases until it breaks.

$(MSe_4)_nI$ phases represent a favorable situation as far as stability of 1D chains is concerned: we are far from the classical ionic pictures in a structure where a metallic chain is enclosed in a selenium frame, and, in addition, the large size of iodine introduces a large separation between chains (6.79 Å, for example, between two metal atoms having the same z value but belonging to different chains in the $(NbSe_4)_3I$ structure). Such a situation can be compared well with the case of Mo_6Se_6 chains of condensed clusters separated by extra cations in $A_2Mo_6Se_6$ derivatives (*8*). In that case replacing Cs^+ by Na^+ or Li^+ reduces the coherence of the structure by making the chains closer. Finally $Li_xMo_6Se_6$ allows us to make dispersion of $(Mo_6Se_6)_n$ chains in some solvents. This could have been

TABLE VIIA

$Nb_4Se_{16}Br_2$

(i) Interatomic distances (Å) within each ($NbSe_8$) polyhedron			
Nb1–Se1	2.567(1)	Nb2–Se1	2.737(1)
–Se2	2.714(1)	–Se2	2.654(1)
–Se3	2.694(1)	–Se3	2.645(1)
–Se12	2.588(1)	–Se12	2.724(1)
Nb1–Se13B	2.505(3)	Nb2–Se4	2.600(1)
–Se13A	2.709(1)	–Se5	2.673(1)
–Se14	2.709(1)	–Se6	2.588(1)
–Se15	2.696(1)	–Se7	2.729(1)
Nb1–Br2	2.661(1)		
Nb3–Se4	2.689(1)	Nb4–Se8	2.546(1)
–Se5	2.570(1)	–Se9	2.733(1)
–Se6	2.674(1)	–Se10	2.741(1)
–Se7	2.611(1)	–Se11	2.554(1)
Nb3–Se8	2.726(1)	Nb4–Se13A	2.624(1)
–Se9	2.637(1)	–Se13B	2.800(4)
–Se10	2.663(1)	–Se14	2.665(1)
–Se11	2.758(1)	–Se15	2.686(1)
		–Se16	2.648(1)
(ii) Interatomic distances (Å) along the metallic chain and between the ($NbSe_4$) chains			
Nb1–Nb2	3.202(1)	Br1–Se5	3.067(1)
Nb2–Nb3	3.076(1)	–Se10	2.950(1)
Nb3–Nb4	3.167(1)	–Se11	3.140(1)
Nb4–Nb1	3.702(1)	–Se15	2.994(1)
		Br2–Se13A	2.998(1)
(iii) Short Se–Se bond lengths			
Se1–Se2	2.333(1)	Se8–Se10	2.375(1)
Se3–Se12	2.370(1)	Se9–Se11	2.355(1)
Se4–Se5	2.389(1)	Se13A–Se16	2.357(1)
Se6–Se7	2.346(1)	Se13B–"Br2"	2.304(4)
		Se14–Se15	2.365(1)

done with $(MSe_4)_nCl$ phases if the ionicity increase due to halogen substitution (a substitution opposite to that of the previous example) had not definitively destabilized the structure.

The two isostructural new compounds $Nb_4Se_{16}Br_2$ and $Ta_4Se_{16}Br_2$, along with $Nb_6Se_{20}Br_6$ (previously published (*6*)), make apparent a continuity scheme between compounds such as NbX_2Y_2 (*9*) and $(MSe_4)_nI$ (*1*) or even VS_4 (*10*). Indeed, they constitute as many extra links in a unitary structural scheme based on a progressive condensation of $[M_2X_4]$ groups. Such $[M_2X_4]$ groups represent rectangular bipyramids in which a strong metal–metal bond corresponding to a short M–M distance (≃ 2.9 Å) span through a selenium rectangle made of two Se–Se pairs (≃ 2.35 Å). In $NbSe_2Cl_2$ or Nb_2Se_9 such bipyramids are iso-

TABLE VIIB

$Ta_4Se_{16}Br_2$

(i) Interatomic distances (Å) within each ($TaSe_8$) polyhedron			
Ta1–Se1	2.558(1)	Ta2–Se1	2.734(1)
–Se2	2.708(1)	–Se2	2.643(1)
–Se3	2.680(1)	–Se3	2.633(1)
–Se12	2.575(1)	–Se12	2.715(1)
Ta1–Se13B	2.506(4)	Ta2–Se4	2.591(1)
–Se13A	2.703(1)	–Se5	2.667(1)
–Se14	2.707(1)	–Se6	2.574(1)
–Se15	2.679(1)	–Se7	2.713(1)
–Br2	2.642(1)		
Ta3–Se4	2.673(1)	Ta4–Se8	2.538(1)
–Se5	2.561(1)	–Se9	2.726(1)
–Se6	2.664(1)	–Se10	2.737(1)
–Se7	2.602(1)	–Se11	2.548(1)
Ta3–Se8	2.716(1)	Ta4–Se13A	2.604(1)
–Se9	2.627(1)	–Se13B	2.718(4)
–Se10	2.565(1)	–Se14	2.649(1)
–Se11	2.744(1)	–Se15	2.685(1)
		–Se16	2.635(1)
(ii) Interatomic distances (Å) along the metallic chain and between the ($TaSe_4$) chains			
Ta1–Ta2	3.187(1)	Br1–Se5	3.048(1)
Ta2–Ta3	3.055(1)	–Se10	2.938(1)
Ta3–Ta4	3.153(1)	–Se11	3.134(1)
Ta4–Ta1	3.683(1)	–Se15	2.993(1)
		Br2–Se13A	2.985(1)
(iii) Short Se–Se bond lengths			
Se1–Se2	2.344(1)	Se8–Se10	2.389(1)
Se3–Se12	2.381(1)	Se9–Se11	2.367(1)
Se4–Se5	2.398(1)	Se13A–Se16	2.348(1)
Se6–Se7	2.359(1)	Se13B–"Br2"	2.352(4)
		Se14–Se15	2.371(1)

lated and separated by chlorine or a Se_5 group, respectively. Partial condensation of $[Nb_2X_4]$ units occur in $Nb_6Se_{20}Br_6$. Two short Nb–Nb bonds ($\simeq$ 3.1 Å) alternate with a longer one (3.94 Å). The shortest bonds are associated with $[Nb_3Se_8]$ groups built up from two $[Nb_2Se_4]$ units. $Nb_4Se_{16}Br_2$ and $Ta_4Se_{16}Br_2$ correspond to a further step in the condensation process: three $[M_2X_4]$ bipyramids are associated in $[M_4X_{12}]$ segments. A long M–M bond separates two successive $[M_4X_{12}]$ associations. An infinite condensation of $[M_2X_4]$ bipyramids leads to VS_4 or $(MSe_4)_nI$ phases. In the first case, long and short V–V bonds alternate along the chains with a $2b$ superstructure, in agreement with a Peierls distortion associated with a half-filled dz^2 band (z direction taken along the chain). In the second case, the presence of iodine in various proportions modulates the sequence of long and short bonds.

$Nb_4Se_{16}Br_2$ and $Ta_4Se_{16}Br_2$ provide support for calculations which, starting from isolated (M_2Se_4) bipyramids, show the progressive formation of a conduction band that will govern the charge density wave instabilities in the (MSe_4) infinite chains of $(MSe_4)_nI$ type phases (*11*). The activation energies observed here have to be associated with the electronic hopping between finite metallic segments.

References

1. P. Gressier, A. Meerschaut, L. Guemas, J. Rouxel, and P. Monceau, *J. Solid State Chem.* **51,** 141 (1984). P. Monceau, M. Renard, J. Richard, M. C. Saint Lager, and Z. Z. Wang, *in* Lecture Notes in Physics. CDW in Solids, Proceedings, Budapest (1984) (Gy Hutiray and J. Solyom, Eds.), Springer-Verlag, New York/Berlin.
2. Z. Z. Wang, P. Monceau, M. Renard, P. Gressier, L. Guemas, and A. Meerschaut, *Solid State Comm.* **47**(6), 438 (1983).
3. P. Delhaes, C. Coulon, S. Flandrois, B. Hilti, C. W. Mayer, G. Rihs, and J. Rivory, *J. Chem. Phys.* **73,** 1452 (1980).
4. D. T. Cromer, and J. T. Waber. "International Tables for X-Ray Crystallography," Vol. IV, Table 2.2A.
5. D. T. Cromer and D. Liberman, *J. Chem. Phys.* **53,** 1891 (1970).
6. A. Meerschaut, P. Grenouilleau, and J. Rouxel, *J. Solid State Chem.* **61,** 90 (1986).
7. M. Evain, M.-H. Whangbo, A. Meerschaut, P. Grenouilleau, P. Gressier, and J. Rouxel, *Inorg. Chem.*, in press.
8. M. Potel, R. Chevrel, M. Sergent, J. C. Armici, M. Decroux, and O. Fischer, *J. Solid State Chem.* **30,** 365 (1979). J. M. Tarascon, G. W. Hull, and F. J. Di Salvo, *Mater. Res. Bull.* **19,** 915 (1984).
9. H. Schäfer and W. Beckmann, *Z. Anorg. Allg. Chem.* **347,** 225 (1966).
10. R. Allmann, I. Baumann, A. Kutoglu, H. Rösch, and E. Hellner, *Naturwissenschaften* **51,** 263 (1964).
11. P. Gressier, M.-H. Whangbo, A. Meerschaut, and J. Rouxel, *Inorg. Chem.* **23**(9), 1221 (1984).
12. K. Yvon, W. Jeitschko, and E. Parthe, *J. Appl. Crystallogr.* **10,** 73 (1977).